Stereoselective Hydrogen Abstraction by Galactose Oxidase[†]

Stefan G. Minasian, Mei M. Whittaker, and James W. Whittaker*

Department of Environmental and Biomolecular Systems, OGI School of Science and Engineering, Oregon Health and Sciences University, 20000 Northwest Walker Road, Beaverton, Oregon 97006

Received July 8, 2004; Revised Manuscript Received August 29, 2004

ABSTRACT: The fungal enzyme galactose oxidase is a radical copper oxidase that catalyzes the oxidation of a broad range of primary alcohols to aldehydes. Previous mechanistic studies have revealed a large substrate deuterium kinetic isotope effect on galactose oxidase turnover whose magnitude varies systematically over a series of substituted benzyl alcohols, reflecting a change in the character of the transition state for substrate oxidation. In this work, these detailed mechanistic studies have been extended using a series of stereospecifically monodeuterated substrates, including 1-*O*-methyl-α-D-galactose as well as unsubstituted benzyl alcohol and 3- and 4-methoxy and 4-nitrobenzyl derivatives. Synthesis of all of these substrates was based on oxidation of the α,α′-dideuterated alcohol to the corresponding ^{2}H-labeled aldehyde, followed by asymmetric hydroboration using α-pinene/9-BBN reagents to form the stereoisomeric alcohols. Products from enzymatic oxidation of each of these substrates were characterized by mass spectrometry to quantitatively evaluate the substrate dependence of the stereoselectivity of the catalytic reaction. For all of these substrates, the selectivity for *pro-S* hydrogen abstraction was at least 95%. This selectivity appears to be a direct consequence of constraints imposed by the enzyme on the orientation of substrates bearing a branched *β*-carbon. Steady state analysis of kinetic isotope effects on *V*/*K* has resolved individual contributions from primary and α-secondary kinetic isotope effects in the reaction, providing a test for the involvement of an electron transfer redox equilibrium in the oxidation process. Multiple isotope effect measurements utilizing simultaneous labeling of the substrate and solvent have contributed to refinement of the relation between proton transfer and hydrogen atom transfer steps in substrate oxidation.

Biological oxidation mechanisms underlie a wide range of processes, including oxygenic photosynthesis (*1*), respiration (*2*), and the interconversion of metabolic intermediates. Oxidation−reduction processes that involve transfer of hydrogen equivalents are especially common, and two classes may be conveniently defined, depending on whether they are based on heterolytic bond cleavage (typically associated with hydride transfer in a polar mechanism) or homolytic bond cleavage (leading to hydrogen atom transfer and a free radical mechanism). The former, heterolytic pathway has been demonstrated in many enzymes that utilize quinone, nicotinamide, or flavin cofactors (*3*−*5*), whereas the latter, homolytic pathway is generally associated with the presence of transition metal ions or redox-active amino acid side chains (e.g., tyrosyl phenoxyl) in the enzyme active site (*6*−*8*). These free radical enzymes have evolved mechanisms for controlling free radicals in catalysis, taking advantage of lower activation barriers that can be accessed through homolytic reaction paths.

Galactose oxidase (*9*−*13*, and references therein), one of the most extensively studied of the free radical enzymes, is a member of the family of radical copper oxidases [that also includes glyoxal oxidase (*14*)] characterized by the presence of a stable metalloradical complex in the active enzyme (*15*)

Scheme 1: Galactose Oxidase Metalloradical Active Site

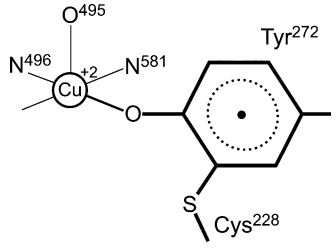

(Scheme 1). The active site is comprised of a copper ion coordinated to a redox-active amino acid side chain (*15*) that has been identified as a tyrosylcysteine (TyrCys) cofactor formed by post-translational cross-linking between a tyrosine (Y272) and a cysteine (C228) residue (*16*). A second tyrosine ligand (Y495) appears to serve as a general base in catalysis (*17*, *18*). The intrinsic redox cofactor in galactose oxidase has been shown to form spontaneously in the precursor protein (*19*) upon addition of Cu(I) and dioxygen in a radical-dependent fashion (*20*). The radical-copper active site serves as a two-electron redox unit, undergoing reduction and oxidation during successive reactions with alcohol and dioxygen in a ping-pong turnover mechanism (*15*, *21*) (Scheme 2). The elements of dihydrogen are transferred from the substrate to the enzyme active site during turnover, forming a reduced Cu(I)−TyrCys nonradical species that is subsequently rapidly reoxidized by dioxygen. One of the hydrogens transferred in the substrate half-reaction is thought to be removed by deprotonation of the coordinated hydroxyl

[†] We gratefully acknowledge support for this project from the National Institutes of Health (Grant GM 46749 to J.W.W.).

* To whom correspondence should be addressed. Telephone: (503) 748-1065. Fax: (503) 748-1464. E-mail: jim@ebs.ogi.edu.

10.1021/bi048554s CCC: $27.50
Published on Web 10/09/2004

Scheme 2: Turnover Reactions for Galactose Oxidase

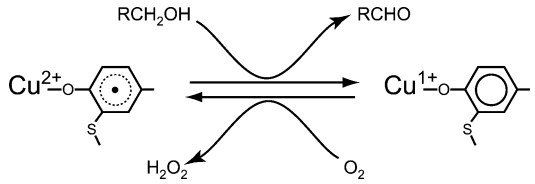

Scheme 3: Stereochemical Assignments of α-Methylene Hydrogens in Galactose Oxidase Substrates

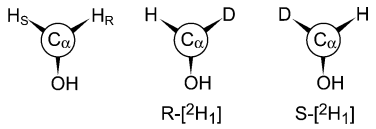

of the substrate (RCH_2OH) by a second coordinated tyrosinate (Y495) in a proton transfer (PT)[1] step, activating the substrate for oxidation. The modified TyrCys side chain in its oxidized, phenoxyl form appears to serve as a hydrogen atom acceptor in the oxidation chemistry, which has been proposed to involve single-electron transfer (SET) and hydrogen atom transfer (HAT) components (*22*).

Galactose oxidase accommodates an unusually broad range of substrate alcohols (*10*,*23*). However, alcohol oxidation is strictly regioselective, and only primary alcohols serve as substrates. For these alcohols, the chiral environment of the enzyme active site allows resolution of the two methylene hydrogens, identified as *pro-R* (H_R) or *pro-S* (H_S) depending on the stereochemical consequence of substitution with a higher-priority atom, e.g., deuterium (Scheme 3). Earlier studies, using partially resolved mixtures of the monodeuterated (6*R*)-6-[^{2}H]galactose and (6*S*)-6-[^{2}H]galactose derivatives, showed that galactose oxidase exhibits a high degree of stereoselectivity for oxidation of the canonical substrate, with preferential abstraction of the *pro-S* hydrogen (*24*), although neither the degree of stereoselectivity of substrate oxidation nor the tacit assumption that the stereoselectivity is independent of the substrate structure has been rigorously tested.

Here we address some of the outstanding mechanistic questions for galactose oxidase substrate oxidation, using isotope methods. Stereospecific deuterium labeling of the α-methylene hydrogens in a series of substrate alcohols (Scheme 4) has allowed us to evaluate the substrate dependence of the reaction stereospecificity, resolve the elementary contributions from *pro-R* and *pro-S* hydrogens in the substrate oxidation transition state for each of these substrates, test alternative reaction mechanisms, and apply multiple simultaneous isotope perturbations to determine the concerted or stepwise character of proton transfer (PT) and hydrogen atom transfer (HAT) steps in substrate oxidation. The alcohols used in these experiments include the canonical substrate, galactose, as well as a series of benzyl alcohol derivatives, including 3-methoxy benzyl alcohol, which is commonly used in galactose oxidase assays, and a set of benzyl alcohol derivatives (benzyl alcohol, 4-methoxy benzyl alcohol, and 4-nitro benzyl alcohol) spanning a broad range of observed substrate deuterium kinetic isotope effects ($k_H/k_D = 4-12$) (*22*). This series of substrates, differing in structure and substitution pattern, have allowed us to investigate the substrate dependence of galactose oxidase stereoselectivity, and gain insight into the structural determinants of stereoselectivity in this enzyme.

[1] Abbreviations: KIE, kinetic isotope effect; SKIE, solvent kinetic isotope effect; PT, proton transfer; SET, single-electron transfer; HAT, hydrogen atom transfer; 9-BBN, 9-borabicyclo[3.3.1]nonane; αMF, *Saccharomyces cerevisiae* α-mating factor leader peptide; gla, *Aspergillus niger* glucoamylase leader peptide.

Scheme 4: Structures of Stereospecifically Deuterated Galactose Oxidase Substrates

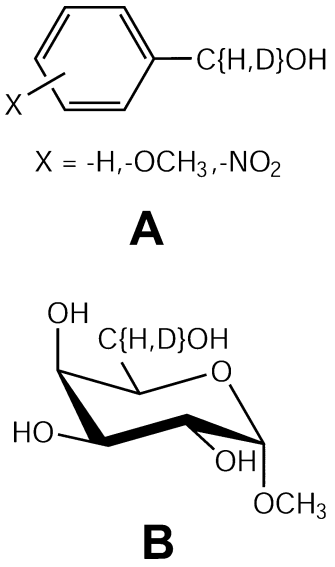

EXPERIMENTAL PROCEDURES

Reagents. All chemicals were purchased from Aldrich and used as received except α-pinene, which was distilled from $LiAlH_4$. Solvents of anhydrous or highest available purity were used. Chromatography medium (Davisil grade 633 silica gel) was obtained from Aldrich.

Synthesis. Unsubstituted, 4-methoxy, and 4-nitro α,α′-dideuterated benzyl alcohols were synthesized by reduction of the corresponding methyl benzoates with $LiAlD_4$ (98 at. % D) (*25*). α,α′-Dideuterated benzyl alcohols were used as the starting materials for asymmetric synthesis of stereospecifically labeled monodeuterated benzyl alcohols. α,α′-Dideuterated benzyl alcohols were converted to benzaldehydes by oxidation with ammonium cerium(IV) nitrate (*26*). The deuterated benzaldehydes were subsequently reduced asymmetrically to the corresponding monodeuterated benzyl alcohols with the (1*S*)-(−)-α-pinene/9-borabicylco[3.3.1]-nonane (9-BBN) adduct [for (*R*)-benzyl-α-[^{2}H]alcohols] or the (1*R*)-(+)-α-pinene/9-BBN adduct [for (*S*)-benzyl-α-[^{2}H]-alcohols] as previously described (*27*, *28*) with slight modifications, as described below.

(R)-Benzyl-α-[^{2}H]alcohol. Methyl benzoate (20.1 g, 148 mmol) in THF (150 mL) was added dropwise to a chilled solution of $LiAlD_4$ (98 at. % D) (4.2 g, 10.0 mmol) in THF (150 mL). After the mixture had been stirred for 2 h, the reaction was quenched and the mixture acidified to pH 1 and extracted. Following purification by distillation, benzyl-α,α′-[$^2H_2$]alcohol (9.0 g, 82 mmol) was suspended in degassed H_2O (300 mL) and heated to 45 °C. Ammonium cerium(IV) nitrate (92 g, 168 mmol) in H_2O (300 mL) was added and allowed to react for 30 min. The aqueous solution was extracted, neutralized, and evaporated. Purification by

simple distillation afforded benz[^{2}H]aldehyde as a clear, pale yellow liquid.

(1*S*)-(−)-α-Pinene (97% ee; 4.70 mL, 29.5 mmol) and 9-BBN (54 mL, 0.5 M in THF) were refluxed under argon for 2 h and cooled to 25 °C. Benz[^{2}H]aldehyde (2.60 g, 24.3 mmol) THF (ca. 5 mL) was added by syringe to the α-pinene/9-BBN solution. The yellow mixture was refluxed for 1 h and cooled to 0 °C, and the reaction was quenched with acetaldehyde (1 mL). Following evaporation, the residue was dissolved in ether and cooled to 0 °C. A white precipitate formed on addition of ethanolamine (1.75 mL, 31.6 mmol), was removed by filtration in a Buchner funnel, and was washed with ether. The ether solution was washed with 1 M KH_2PO_4 to efficiently remove traces of the amine, dried with $MgSO_4$, and distilled to yield a clear, colorless liquid (1.41 g, 53.1%): ^{1}H NMR ($CDCl_3$, reference $CHCl_3$) δ 7.34 (m, 4H), 7.28 (m, 1H), 4.64 (s, 1H), 1.87 (s, 1H).

(S)-Benzyl-α-[^{2}H]alcohol. Preparation was exactly the same as with the (*R*) enantiomer, except 2.23 g (20.4 mmol) of the aldehyde was used, along with appropriate amounts of the other reagents, including (1*R*)-(+)-α-pinene (97% ee) to direct the stereospecific reduction. Purification by simple distillation afforded a clear, colorless liquid (1.36 g, 61.1%): ^{1}H NMR ($CDCl_3$, reference $CHCl_3$) δ 7.34 (m, 4H), 7.28 (m, 1H), 4.64 (s, 1H), 1.86 (s, 1H).

Reaction progress was monitored by thin-layer chromatography, using a 1:1 hexane/ethyl acetate mixture as the developing solvent. The products were purified by vacuum distillation or by a combination of silica gel chromatography and vacuum distillation. Enantiomeric purities of all products were evaluated by esterifying the α-monodeuterated alcohols with (*S*)-(+)-*O*-acetylmandelic acid (98% ee) and integrating the resolved peaks assigned to the two diastereotopic α-methylene protons in the ^{1}H NMR spectrum (*29*). NMR spectra were recorded at ambient temperature on a Bruker Advance-400 spectrometer. Stereospecifically monodeuterated 4-methoxy, 4-nitro, and 3-methoxy benzyl alcohols were synthesized by the same procedure except dideuterated 3-methoxy benzyl alcohol was oxidized with pyridinium chlorochromate (*30*) to the corresponding [^{2}H]aldehyde prior to reduction with the α-pinene/9-BBN reagent.

Stereospecifically monodeuterated 1-*O*-methyl-D-(+)-galactopyranosides were prepared from 1,6-dimethyl-D-galacturonic acid (**1**) in a five-step synthetic procedure, as described below. Commercial galacturonic acid was converted to 1,6-dimethyl-α-D-galacturonate ester as previously described (*31*). 1-*O*-Methyl-6,6′-di[^{2}H]-α-D-(+)-galactopyranoside was prepared by reduction of 1,6-dimethyl-α-D-galacturonate ester by $NaBD_4$ as previously described (*21*, *32*).

*2,3,4-Tris(tert-butyldimethylsilyl)-1,6-dimethyl-α-D-galacturonate Ester (**2**)*. 1,6-Dimethyl-α-D-galacturonate ester **1** (24.7 g, 0.104 mol) was suspended in CH_2Cl_2 (500 mL) and exposed to *tert*-butyldimethylsilyl trifluoromethanesulfonate (211 g, 0.800 mol) and 2,6-lutidine (120 mL, 1.03 mol) (*33*) for 15 min before the reaction was quenched with methanol. The mixture was diluted with CH_2Cl_2, washed with 0.1 M HCl and saturated $NaHCO_3$, dried with $MgSO_4$, and evaporated. The residue was reserved for use in the next step without further purification: ^{1}H NMR ($CDCl_3$, reference $CHCl_3$) δ 4.76 (d, 1H, J = 3.5 Hz), 4.38 (d, 1H, J = 1.3 Hz), 4.21 (dd, 1H, J = 2.9, 1.5 Hz), 3.99 (dd, 1H, J = 9.6, 3.5 Hz), 3.87 (dd, 1H, J = 9.6, 2.9 Hz), 3.78 (s, 3H), 3.41 (s, 3H), 0.91 (s, 18H), 0.88 (s, 9H), 0.14 (s, 3H), 0.10 (m, 9H), 0.08 (s, 3H), 0.07 (s, 3H).

*1-O-Methyl-2,3,4-tris(tert-butyldimethylsilyl)-6,6′-di[^{2}H]-α-D-galactopyranoside (**3**)*. $LiAlD_4$ (98 at. % D) (7.27 g, 173 mmol) was added slowly to a chilled solution of **2** in THF (2 L). The internal temperature was kept below −5 °C during the addition, and then stirred for an additional 10 min to complete the reaction. The mixture was diluted with ether, washed consecutively with 0.1 M HCl and saturated $NaHCO_3$, dried with $MgSO_4$, and evaporated for immediate use: ^{1}H NMR ($CDCl_3$, reference $CHCl_3$) δ 4.72 (d, 1H, J = 3.0 Hz), 4.0 (m, 2H), 3.93 (dd, 1H, J = 8.76, 2.33 Hz), 3.81 (s, 1H), 3.39 (s, 3H), 0.96 (s, 9H), 0.94 (s, 9H), 0.94 (s, 9H), 0.18 (s, 3H), 0.17 (s, 3H), 0.15 (s, 3H), 0.13 (s, 3H), 0.12 (s, 3H), 0.12 (s, 3H).

*1-O-Methyl-2,3,4-tris(tert-butyldimethylsilyl)-6-[^{2}H]-α-D-galactopyran-6-aldehyde (**4**)*. CrO_3 was added slowly to a chilled solution of pyridine (190 mL, 2.36 mol) in CH_2Cl_2 and the mixture stirred at −10 °C for 1 h. A solution of **3** in CH_2Cl_2 was added, and the mixture was stirred for 12 h while warming to room temperature. Filtration through silica gel and evaporation afforded the aldehyde which was used immediately without further purification: ^{1}H NMR ($CDCl_3$, reference $CHCl_3$) δ 4.87 (d, 1H, J = 1.7 Hz), 4.53 (br, 1H), 4.09 (d, 1H, J = 5.4 Hz), 3.87 (dd, 1H, J = 5.7, 2.1 Hz), 3.78 (m, 1H), 3.53 (s, 3H), 0.91 (s, 18H), 0.88 (s, 9H), 0.14 (s, 3H), 0.10 (m, 9H), 0.08 (s, 3H), 0.07 (s, 3H).

*1-O-Methyl-2,3,4-tris(tert-butyldimethylsilyl)-(6R)-6-[^{2}H]-α-D-galactopyranoside (**5**)*. (1*S*)-(−)-α-Pinene (6.8 mL, 42.7 mmol) and 9-BBN (80 mL, 0.5 M in THF) were refluxed for 2 h and then cooled to room temperature. **4** (17.5 g, 32.2 mmol) was dissolved in a small amount of THF and added by syringe to the α-pinene/9-BBN solution. The yellow mixture was brought to reflux for an additional 1 h and then cooled to 0 °C and the reaction quenched with acetaldehyde. After evaporation of the volatiles, the residue was redissolved in ether and cooled to 0 °C. A white precipitate formed upon addition of ethanolamine (1.75 mL, 31.6 mmol), which was removed by filtration. The ether solution was washed with KH_2PO_4 (1.0 M in H_2O), dried with $MgSO_4$, and evaporated: ^{1}H NMR ($CDCl_3$, reference $CHCl_3$) δ 4.72 (d, 1H, J = 2.98 Hz), 4.01 (m, 2H), 3.93 (dd, 1H, J = 8.8, 2.3 Hz), 3.81 (m, 2H), 3.38 (s, 3H), 0.92 (s, 9H), 0.91 (s, 9H), 0.91 (s, 9H), 0.15 (s, 3H), 0.14 (s, 3H), 0.11 (s, 3H), 0.09 (s, 3H), 0.08 (s, 3H), 0.07 (s, 3H).

*1-O-Methyl-2,3,4-tris(tert-butyldimethylsilyl)-(6S)-6-[^{2}H]-α-D-galactopyranoside (**6**)* was generated by following the procedure for the preparation of **5**, using (1*R*)-(+)-α-pinene: ^{1}H NMR ($CDCl_3$, reference $CHCl_3$) δ 4.71 (d, 1H, J = 2.99 Hz), 4.01 (m, 2H), 3.93 (dd, 1H, J = 8.8, 2.3 Hz), 3.83 (m, 2H), 3.38 (s, 3H), 0.92 (s, 9H), 0.91 (s, 9H), 0.91 (s, 9H), 0.15 (s, 3H), 0.14 (s, 3H), 0.11 (s, 3H), 0.09 (s, 3H), 0.08 (s, 3H), 0.07 (s, 3H).

*1-O-Methyl-(6R)-6-[^{2}H]-α-D-galactopyranoside (**7**)*. Dowex 50W X2−400 (ca. 220 g) was added to a solution of **5** (12.0 g, 22.0 mmol) in methanol (200 mL), and the mixture was stirred at room temperature for 16 h. The mixture was filtered, washed with hexane, and concentrated. The final product crystallized after the mixture had stood at a reduced temperature for several days: ^{1}H NMR (D_2O, reference HDO) δ 4.86 (d, 1H, J = 2.9 Hz), 3.99 (m, 1H), 3.92 (d,

1H, $J = 4.2$ Hz), 3.84 (m, 2H), 3.75 (d, 1H, $J = 4.1$ Hz), 3.44 (s, 3H).

*1-O-Methyl-(6S)-6-[^{2}H]-α-D-galactopyranoside (**8**)* was prepared by following the procedure for the preparation of **7**, from **6**: ^{1}H NMR (D_2O, reference HDO) δ 4.86 (dd, 1H, $J = 2.7$, 0.5 Hz), 3.99 (m, 1H), 3.92 (dt, 1H, $J = 8.2$, 0.5 Hz), 3.84 (m, 2H), 3.76 (d, 1H, $J = 8.2$ Hz), 3.44 (s, 3H).

The isomeric purity of the monodeuterated sugars was evaluated by ^{1}H NMR analysis of the products, integrating the resolved peaks arising from the two stereochemically distinct α-hydrogens.

Biological Materials. Recombinant galactose oxidase (EC 1.1.3.9) was purified from high-density methanol fermentation medium (*34*, *35*) of *Pichia pastoris* transformants prepared by multicopy chromosomal integration of an expression cassette comprising the pPICZ Zeocin-selection plasmid (Invitrogen) with either the *Aspergillus niger* glucoamylase leader peptide (Gla) (*36*) or the *Saccharomyces cerevisiae* α-mating factor leader peptide (αMF) (*20*) spliced with the cDNA sequence encoding the galactose oxidase protein. The galactose oxidase concentration was determined by optical absorption measurements, using the previously reported molar extinction coefficient [$\epsilon_{280} = 1.05 \times 10^5$ M^{-1} cm^{-1}] (*37*). Bovine liver catalase (EC 1.11.1.6) was purchased from Sigma. Protocatechuate 3,4-dioxygenase (EC 1.13.11.3) was isolated from *Brevibacterium fuscum* as previously described (*38*). Deuterium oxide (99.9 at. % D) was from Aldrich.

Biochemical Methods. Galactose oxidase activity was measured using a thermostated (25 °C) Clark oxygen electrode attached to a high-accuracy polarographic amplifier (*21*). Reactions were carried out in 50 mM air-saturated sodium phosphate buffer (pH 7.0) with 5 mM 1-*O*-methyl-α-D-galactopyanoside or benzyl alcohol substrate in the presence of 2 mM $K_3Fe(CN)_6$. For absolute rate measurements, the response of the Clark oxygen electrode was calibrated by stoichiometric oxidation of 0.1 μmol of protocatechuic acid by protocatechuate 3,4-dioxygenase (*39*). For isotope effect measurements, protio, monodeuterio, and dideuterio forms of a given substrate were assayed in parallel. Benzyl alcohol substrates were dissolved in assay buffer by sonication, and the concentrations of the samples were checked by UV absorption spectroscopy. Slight differences in the substrate concentration detected by absorption spectroscopy were typically normalized by adjusting the volumes of the substrate stock solution in the assay mixture according to the observed sample UV intensity. For solvent isotope effect measurements, reactions in D_2O were set up using enzyme and substrates dissolved in buffered D_2O, with the pD of the solution defined by the composition of the buffer salts. For mass analysis of turnover products of the benzyl alcohol substrates, 2 mL of the assay mixture containing 0.2 mg of galactose oxidase and 500 units of bovine catalase was incubated overnight at 30 °C in a shaking water bath. The reaction mixture was heated in boiling water for 2 min and centrifuged for 10 min to precipitate the protein, and the product was extracted with methylene chloride for mass analysis. For analysis of sugar oxidation products, 50 mM 1-*O*-methyl-α-D-galactopyranoside, 0.2 mg of galactose oxidase [for 6,6′-[H_2]galactose and (6*R*)-6-[^{2}H]galactose] or 2 mg of galactose oxidase [for (6*S*)-6-[^{2}H]galactose and 6,6′-[$^2H_2$]galactose], and 1000 units of catalase were present in the 2 mL reaction mixture. After incubation at 30 °C for 24 h, the reaction mixture was heated in boiling water for 2 min and centrifuged for 10 min to precipitate the protein, and the supernatant containing 1-*O*-methyl-D-galactose-6-aldehyde was concentrated by lyophilization. The aldehyde product was converted to the trimethylsilyl derivative for mass analysis (*40*). Mass spectral analysis was performed using a Perkin-Elmer TurboMass Gold GC/MS instrument for chemical ionization (CI+) using methane as the reagent gas.

Table 1: Summary of ^{1}H NMR Data Used To Determine the Isomeric Purity of Substrates

		major peak[a]		minor peak[a]		
substrate	isomer	chemical shift (δ)	area	chemical shift (δ)	area	isomeric purity[b] (%)
4-H	*R*	5.162	370	5.102	19.5	97
4-H	*S*	5.106	394	5.166	11.0	99
4-NO_2	*R*	5.242	70.5	5.225	3.58	97
4-NO_2	*S*	5.225	100.0	5.24	6.5	96[c]
4-OCH_3	*R*	5.109	846	5.032	52.3	96
4-OCH_3	*S*	5.031	813	5.109	39.8	97
galactose	*R*	3.75	20.3	3.76	1.8	94
galactose	*S*	3.76	18.0	nd[d]	nd[d]	100

[a] ^{1}H NMR resonance for α-methylene hydrogens of the monodeuterated alcohols. Benzyl alcohols were analyzed as (*S*)-(+)-*O*-acetylmandelic acid esters prepared as described in Experimental Procedures. [b] Minimum values, estimated by dividing the area of the major diastereotopic α-methylene proton resonance by the sum of both α-methylene proton resonances, after correcting each of the values for the predicted presence of 2% of the diprotio form in the product. [c] Integration determined manually; the peak corresponding to the minor diastereotopic α-methylene proton resonance was not resolved by automated Lorentzian line fit analysis. [d] Not detected.

RESULTS AND DISCUSSION

Characterization of Labeled Substrates. The molecular, isotopic, and isomeric purity of the labeled substrates was evaluated by ^{1}H NMR and corrected for a small fraction (2%) of diprotio product predicted based on the ^{1}H present in the 98 at. % D $LiAlD_4$ reductant used in the synthetic procedures (Table 1). Similarly small (1.5%) enantiomeric impurities in the α-pinene chiral agents used to direct the stereochemistry of the α-monodeuterated alcohols and a 1% enantiomeric impurity in the chiral resolution reagent (*O*-acetylmandelic acid) used to analyze the product stereochemistry can account for the observed (real or apparent) defects in the enantiomeric purity of each of the benzyl alcohol products. The results, shown in Table 1, reflect the well-established high degree of stereoselectivity afforded by the α-pinene/9-BBN reagent (*27*, *28*, *41*). Assignment of absolute stereochemistry of the monodeuterated benzyl alcohol derivatives was based on both the preferred stereochemistry of the α-pinene/9-BBN reduction (*27*, *28*) and ^{1}H NMR chemical shift correlations for the *O*-acetyl mandelate esters (*29*).

The synthesis of stereochemically defined monodeuterated galactose derivatives followed a novel approach that is somewhat more straightforward than the previously reported method (*42*), allowing for parallel synthesis of both (6*R*) and (6*S*) stereoisomers. The assignment of absolute stereochemistry for the diastereomeric α-monodeuterated products was based on the previously reported ^{1}H NMR characterization

Table 2: Mass Spectral Data for Oxidation Products

substrate	isotopomer[a]	product mass relative intensities (%)[b] *m/z* 106	*m/z* 107	*m/z* 108	*m/z* 109
benzyl alcohol	HH	4.3 ± 1.9	100	**7.1 ± 0.2**	
	SD	7.6 ± 1.7	100	**13.1 ± 0.3**	
	RD		**29.1 ± 0.7**	100	7.64 ± 0.05
	DD		**16.3 ± 1.9**	100	7.6 ± 0.3

substrate	isotopomer[a]	product mass relative intensities (%)[b] *m/z* 151	*m/z* 152	*m/z* 153	*m/z* 154
4-NO_2 benzyl alcohol	HH	2.6 ± 0.5	100	**4.9 ± 0.5**	
	SD	2.3 ± 0.6	100	**9.1 ± 0.9**	
	RD		**3.9 ± 0.2**	100	7.9 ± 0.1
	DD		**4.4 ± 0.3**	100	7.5 ± 0.1

substrate	isotopomer[a]	product mass relative intensities (%)[b] *m/z* 136	*m/z* 137	*m/z* 138	*m/z* 139
4-OCH_3 benzyl alcohol	HH	26.8 ± 0.5	100	**5.7 ± 0.4**	
	SD	26.3 ± 1.1	100	**10.6 ± 0.4**	
	RD		**36.0 ± 0.5**	100	6.7 ± 0.4
	DD		**33.1 ± 0.3**	100	7.1 ± 0.4

substrate	isotopomer[a]	product mass relative intensities (%)[b] *m/z* 136	*m/z* 137	*m/z* 138	*m/z* 139
3-OCH_3 benzyl alcohol	HH	42.3 ± 0.3	100	**5.4 ± 0.4**	
	SD	40.7 ± 0.2	100	**7.4 ± 0.1**	
	RD		**42.8 ± 0.3**	100	5.3 ± 0.1
	DD		**45.8 ± 1.0**	100	5.2 ± 0.2

substrate	isotopomer[a]	product mass relative intensities (%)[b] *m/z* 409	*m/z* 410	*m/z* 411	*m/z* 412
1-*O*-methyl-α-D-galactopyranoside	HH	100	**32.5 ± 0.9**	16.9 ± 1.1	
	SD	100	**35.6 ± 1.3**	15.8 ± 2.1	
	RD	**7.7 ± 2.3**	100	33.0 ± 1.0	17.1 ± 0.9
	DD	**6.8 ± 1.8**	100	31.7 ± 1.9	15.7 ± 0.6

[a] HH, α,α′-di-[^{1}H]; SD, (*S*)-α-[^{2}H]; RD, (*R*)-α-[^{2}H]; DD, α,α′-di-[^{2}H]. [b] GC−MS CI+ data using methane reagent gas as described in Experimental Procedures, without correction for enantiomeric and isotopic purity. [c] The intensity values shown in boldface type are predicted to be equal within pairs of products (HH and SD, RD and DD) for strictly stereospecific atom abstraction following correction for enantiomeric and isotopic purity, as described in Product Analysis in the Results and Discussion.

of these compounds (*43*). Subtle differences in chemical shifts found for the 6-^{1}H atoms (but not others) in the monodeuterated galactose derivatives compared to the diprotio form ($\Delta\delta < 0.02$ ppm) may reflect chemical shift isotope effects that are well-known to occur in the ^{1}H NMR of polyatomic molecules, as a result of either geminal electronic perturbations or deuterium isotope effects on conformational equilibria (*44*). The ^{1}H NMR analysis also provides evidence for a small amount (<6%) of (6*S*)-6-[^{2}H$_1$]galactose in the (6*R*) product (Table 1), suggesting a slight relaxation of the stereospecificity of the asymmetric hydroboration reaction in the presence of steric congestion associated with nearby stereocenters. Reduction of the *re* and *si* faces of the galactose-6-aldehyde by (*R*)- and (*S*)-pinene reagents would occur via four distinct diastereomeric transition states, so there is no symmetry constraint on the reaction preference in this case. The fact that none of the alternate isomer is present in the (6*S*)-6-[^{2}H$_1$]galactose product is consistent with the previously observed pattern of stereoselectivity for *si* and *re* face reduction of galactose-6-aldehyde with achiral reductants (*24*).

Product Analysis. Isotopic distributions in the enzyme turnover products of α-monodeuterio substrates were evaluated by GC−MS using chemical ionization (CI+) methods (Table 2). Products of enzymatic oxidation of α,α′-diprotio and α,α′-dideuterio substrates were run in parallel as calibration standards. CI+ mass spectra for the benzyl alcohol oxidation products are dominated by the protonated molecular ion peak ($m/z = M + 1$) (Figure 1). The spectra also include the predicted M + 2 ^{13}C enrichment peak (^{13}C, 1.11% natural abundance, isotopic peak intensity predicted to be 7.7% of the molecular ion peak for benzyl alcohol). In addition, characteristic fragmentation products are observed at lower masses, including a significant peak near *m/z* 79 for the parent benzyl alcohol corresponding to loss of the aldehyde carbonyl with transfer of the aldehydic hydrogen to the ring system. The products formed by oxidation of diprotio and dideuterio alcohols exhibit the expected 1 mass unit difference in *m/z* for the major ion peak. Comparison of the mass spectra for the products of all four isomeric and isotopic forms of the benzyl alcohol derivatives (Table 2) demonstrates a high degree of stereoselectivity for the

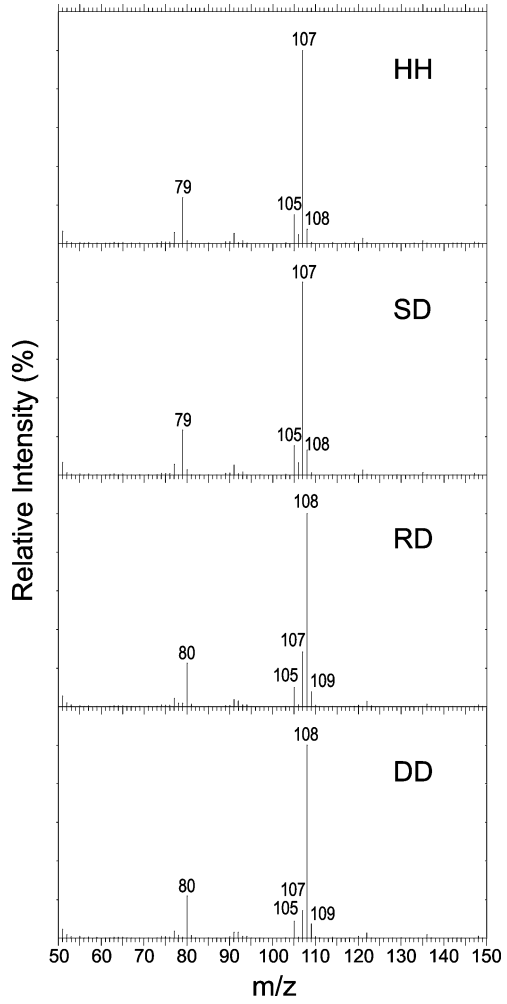

FIGURE 1: Mass spectra for products of oxidation of benzyl alcohols by galactose oxidase: HH, α,α′-[$^1H_2$]benzyl alcohol oxidation product; SD, α-(*S*)-[$^2H_1$]benzyl alcohol oxidation product; RD, α-(*R*)-[$^2H_1$]benzyl alcohol oxidation product; DD, α,α′-[$^2H_2$]benzyl alcohol oxidation product. Samples were prepared as described in Experimental Procedures and analyzed by GC−MS CI+ using methane as the reagent gas.

oxidation step is maintained over this entire set of alternative substrates. If the reactions were performed with 100% stereoselectivity, the mass spectra of diprotio (HH) and (*S*)-[^2H] (SD) oxidation products would be expected to be identical, after correction for enantiomeric and isotopic purity, as would the mass spectra of dideuterio (DD) and (*R*)-[^2H] (RD) oxidation products. If the reaction were completely unselective, on the other hand, the oxidation products of the SD and RD stereoisomers would be identical, with a pair of ion peaks of nearly equal intensity differing by a single mass unit, while the HH and DD products would be the same as for 100% stereoselective oxidation. The experimental results for 4-nitro benzyl alcohol, 3-methoxy benzyl alcohol, and 4-methoxy benzyl alcohol are very close to the ideal limit for complete stereoselectivity. The results for benzyl alcohol suggest the possibility of a slight relaxation of stereoselectivity for oxidation of this simplest congener, perhaps a consequence of less steric hindrance for the unsubstituted ring system; however, the maximum amount of the alternative oxidation stereochemistry allowed by these results is still only ∼5%. This analysis is also consistent with the pattern of intensities observed in the carbonyl fragmentation region (M − 27) of the mass spectra.

The products of oxidation of galactose derivatives by galactose oxidase were also analyzed by GC−MS CI+ methods following derivatization with trimethylsilyl chloride (*40*) (Table 2). The mass spectra of the silylated sugar derivatives reflect contributions from natural abundance ^{13}C (for the $C_{16}H_{36}O_6Si_3$ molecule) as well as silicon isotopes (^{29}Si, 4.68% natural abundance; ^{30}Si, 3.09% natural abundance). The predicted isotopic abundances result in a pattern of intensities with a predominant M + 1 ion peak (100%) at *m*/*z* 409 (for the [^1H]aldehyde) or *m*/*z* 410 (for the [^2H]-aldehyde product) together with significant M + 2 (32.8%) and M + 3 (16.2%) intensities. This pattern is evident in the CI+ mass spectral data (Table 2). The analysis of the patterns observed for HH, RD, SD, and DD oxidation products is identical to that followed for the benzaldehydes (*vide infra*) and provides strong evidence for nearly exclusive *pro-S* hydrogen abstraction from the 6-methylene group of galactose by galactose oxidase. These results represent a stringent test of the stereoselectivity of the galactose oxidase catalytic chemistry. Similar methods have recently been applied in investigating the stereoselectivity of substrate oxidation by the quinohemoprotein amine dehydrogenase (*45*).

The strong stereoselectivity expressed in the oxidation of substrate by galactose oxidase implies that the enzyme strictly constrains the orientation of the substrate in the active site. Inspection of the structure of galactose oxidase (PDB entry 1gog) reveals a shallow channel through which substrates in solution may reach the catalytic site (Figure 2), bounded by Phe194, Phe464, R330, and W290 and opening asymmetrically above the metal complex. Modeling galactose into the crystal structure of the native enzyme, with the 6-hydroxyl coordinated to copper as previously proposed for the catalytic complex (*12*, *13*), leads to severe steric interference except for orientations that permit the pyranose ring to project out through this channel (Figure 3). Similar results have been reported in theoretical studies of the substrate complex (*46*, *47*). This conformation constrains the Cu−O−C_α−C_β torsion angle ω to ∼100° (Scheme 5), bringing the *pro-S* α-hydrogen within hydrogen bonding distance (approximately 2.5 Å) of the TyrCys phenoxyl oxygen while projecting the *pro-R* hydrogen away from the cofactor (Figure 3). The geometry of this complex can account for the observed *pro-S* stereoselectivity of hydrogen abstraction, with the TyrCys phenoxyl playing the role of hydrogen acceptor. The steric constraints that lead to this stereoselectivity are not limited to pyranose sugars, and in fact, we expect similar selectivity will be demonstrated for any substrate bearing a branched C_β, including benzyl alcohols and other substrates having two sterically demanding atoms (C, N, O, etc.) at C_β. This prediction is supported by the observed stereoselectivity of the benzyl alcohol series of substrates, which share a branched C_β as a selectivity determinant. Substrates that permit greater rotational flexibility in the torsion angle ω would be predicted to exhibit lower stereoselectivity on the basis of this analysis. The constraints imposed on substrate binding geometry that are reflected in the stereoselectivity of the turnover reaction may also make significant contributions to catalytic rate enhancement, since a rigid and well-defined orientation of the substrate hydroxyl group is likely

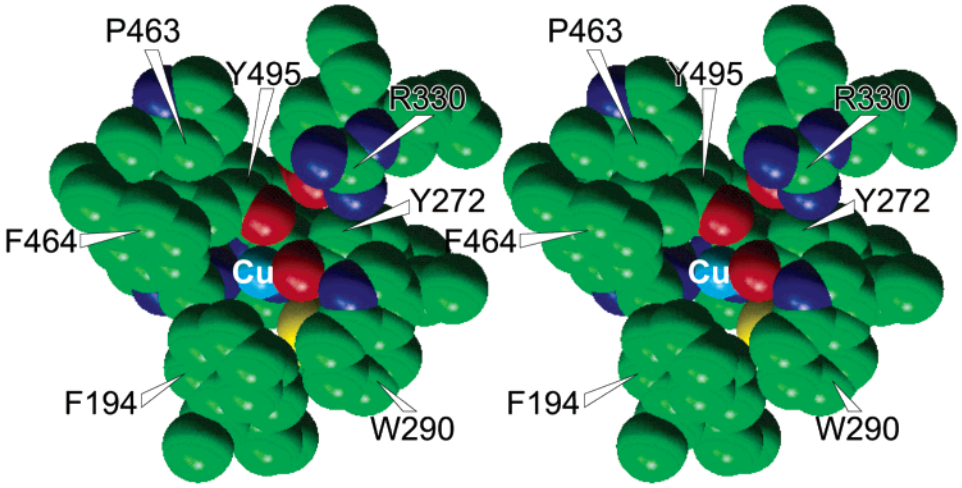

FIGURE 2: Space-filling stereoview of the extended active site of galactose oxidase. The active site copper ion (Cu) and directly coordinated amino acid side chains (Tyr272−Cys228 redox cofactor, Tyr495, His496, and His581) are shown in the context of the outer sphere residues (Phe194, Trp290, Arg330, Pro463, and Phe464) which define the substrate access channel. The structure is based on PDB entry 1gog and rendered with InsightII.

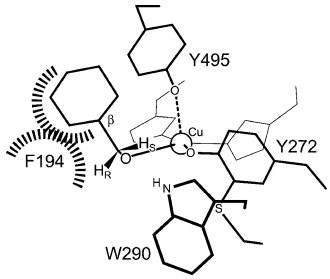

FIGURE 3: Steric constraints on substrate binding geometry in the galactose oxidase active site. A primary alcohol bearing a branched C_β is shown modeled into the galactose oxidase active site, illustrating the steric conflicts with channel residues (Phe194) which restrict the orientation of the substrate in the enzyme complex. The diastereotopic *pro-R* (H_R) and *pro-S* hydrogens (H_S) are identified.

Scheme 5: Methylene Torsion Angle in the Substrate Complex

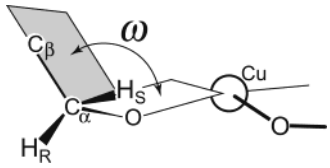

to be important for efficient atom transfer in the oxidation mechanism. Atom transfer processes are known to depend strongly on the geometry of the complex, being favored by proximity and in-line geometry for the atom transfer reaction coordinate (*48*).

Substrate Kinetic Isotope Effect. The analysis of stereoselectivity of substrate oxidation by galactose oxidase is an essential step in analysis of the kinetic isotope effects for the stereoisomeric monodeuterated substrates, since interpretation of the kinetic data in terms of primary or α-secondary isotope effects presumes knowledge of the reaction stereochemistry. Reaction rates measured for the series of stereospecifically monodeuterated substrates, including 3- or 4-substituted benzyl alcohols and 1-*O*-methyl-α-D-galactopyranoside (Table 3), demonstrate a dramatic sensitivity to the stereochemistry of the isotopic labeling. In all cases, the (*R*) isomer (in which the *pro-R* hydrogen of the alcohol α-methylene group is replaced with deuterium) supports a faster oxidation rate than the (*S*) isomer (Table 3, columns 3 and 4). For this set of substrates, the (*R*) isomers are oxidized 3−10 times faster than the corresponding (*S*) isomers. The strong selectivity between isomeric isotopic substrates implies a significant stereoselectivity associated with substrate oxidation, consistent with the mass spectral data (*vide infra*). This selectivity is also reflected in the variation in deuterium isotope effects measured on *V*/*K* observed for the stereochemically distinct α-monodeuterated and the α,α′-dideuterated substrates (Table 3, columns 6−8). The product analysis (*vide supra*) allows us to identify the KIEs associated with (*S*) and (*R*) deuteriation as resolved primary and α-secondary substrate deuterium kinetic isotope effects, α(1) and α(2). The primary deuterium KIE [α(1)] arises from the isotopic substitution of the atom transferred from the methylene position of the alcohol during oxidation, while the α-secondary deuterium KIE [α(2)] arises from isotopic substitution of the nontransferred hydrogen, which is retained in the product (*49*, *50*). Even though the bond to the nontransferred hydrogen is not broken in the transition state, the change in bonding associated with rehybridization at the α-carbon (sp^3 to sp^2) during oxidation of the alcohol to aldehyde is expected to result in a substantial α-secondary kinetic isotope effect. The values of α(2) found experimentally (Table 3) range from 1.19 to 1.44, all of which are consistent with the range of values predicted by theory (1.1−1.4) (*50*), but range toward the higher limit, a trend that reflects substantial rehybridization at Cα during C−H bond cleavage and may be interpreted as indicating quantum mechanical tunneling of the hydrogen (*51*). The magnitudes of the primary kinetic isotope effects are large, but clearly lower than the overall values observed with dideuterated substrates, which correspond to the product of primary and secondary isotope effects [α(1) × α(2)].

An alternative interpretation of the kinetic isotope effects in the galactose oxidase reaction has been suggested, involving a contribution from a partially rate-limiting electron transfer redox equilibrium (SET) in the substrate oxidation step (*21*) (Figure 4). Oxidation of an alcohol to an alkoxyl free radical also affects the bonding within the methylene group, affecting both C−H bonds equally and resulting in

Table 3: Kinetic Parameters for Oxidation of α,α′-Diprotio, α-Monodeuterio, and α,α′-Dideuterio Substrates by Galactose Oxidase

substrate	k_{HH} (M^{-1} s^{-1})[a]	k_{RD} (M^{-1} s^{-1})	k_{SD} (M^{-1} s^{-1})	k_{DD} (M^{-1} s^{-1})	$(k_{HH}/k_{DD})_{obs}$	$(k_{HH}/k_{RD})_{obs}$[b]	$(k_{HH}/k_{SD})_{obs}$[c]	$(k_{HH}/k_{RD})_{obs} \times (k_{HH}/k_{SD})_{obs}$
benzyl alcohol	363 ± 4	272 ± 2	68.3 ± 0.7	51.6 ± 0.5	7.05 ± 0.13	1.34 ± 0.02	5.32 ± 0.08	7.13 ± 0.2
4-nitro benzyl alcohol	326 ± 3.5	260 ± 4.5	30.7 ± 0.6	27.2 ± 0.6	12.0 ± 0.3	1.25 ± 0.03	10.6 ± 0.2	13.3 ± 0.4
4-methoxy benzyl alcohol	487.3 ± 6	408 ± 10	138.6 ± 2	116.4 ± 3	4.19 ± 0.1	1.19 ± 0.03	3.52 ± 0.07	4.19 ± 0.1
3-methoxy benzyl alcohol	4472 ± 22	3522 ± 9	1163 ± 3	980 ± 12	4.57 ± 0.06	1.27 ± 0.01	3.85 ± 0.08	4.89 ± 0.1
1-*O*-methyl-α-D-galactopyranoside	29466 ± 500	20484 ± 300	2242 ± 60	1632 ± 10	18.0 ± 0.33	1.44 ± 0.03	13.1 ± 0.4	18.9 ± 0.7

[a] Measured polarographically at 25 °C as described in Experimental Procedures. [b] Experimental α-secondary deuterium kinetic isotope effect, α(2). [c] Experimental primary deuterium kinetic isotope effect, α(1).

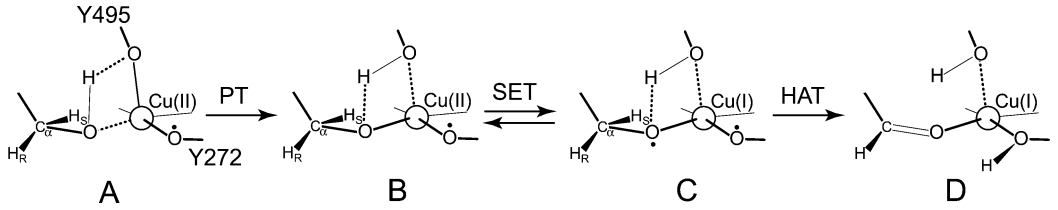

FIGURE 4: Proposed mechanism for alcohol oxidation by galactose oxidase. (A) Substrate binding results in formation of a hydrogen bond between the coordinated hydroxyl group and the Tyr495 phenolate and constrains H_S to a position close to the Tyr272 phenoxyl oxygen. (B) Proton transfer (PT) involving Tyr495 as a general base activates the substrate for oxidation. (C) An unfavorable single-electron transfer (SET) redox equilibrium generates an alkoxyl complex. (D) Hydrogen atom transfer (HAT) to the phenoxyl free radical acceptor results in formation of the aldehyde product. This figure is based on PDB entry 1gog and rendered with InsightII.

an equilibrium deuterium isotope effect on electron transfer. We have previously indicated that the anomalously large substrate deuterium KIE observed for α,α′-dideuterated galactose can be ascribed to a modest primary KIE ($k_H/k_D \sim 10$) combined with an isotope fractionation factor ($1/\beta$) of 0.8 (per deuterium) on a prior unfavorable electron transfer equilibrium. These effects occur within the same catalytic step and are multiplicative (*52*−*54*), so the overall observed effect (involving an unfavorable equilibrium) is the product of three terms (eq 1):

$$(k_{HH}/k_{DD})_{obs} = \alpha(1) \times \alpha(2) \times (2\beta - 1) \quad (1)$$

where α(1) is the primary deuterium kinetic isotope effect, α(2) is the α-secondary kinetic isotope effect, and β is the reciprocal fractionation factor for the deuterium isotope effect on the (unfavorable) electron transfer equilibrium ($K_{eq,H}/K_{eq,D}$). The factor $2\beta - 1$ includes the correction for the presence of two isotopic nuclei. For the monodeuterated substrates, one of the kinetic isotope effect terms or the other vanishes, and the fractionation factor is reduced to the value for a single deuterium nucleus (eqs 2 and 3):

$$(k_{HH}/k_{RD})_{obs} = \alpha(2) \times \beta \quad (2)$$

$$(k_{HH}/k_{SD})_{obs} = \alpha(1) \times \beta \quad (3)$$

To evaluate these data, we have defined an empirical parameter γ, the ratio of the observed isotope effect for the dideuterated substrate to the product of observed isotope effects for (*R*) and (*S*) monodeuterated substrates (eq 4):

$$\gamma = (k_{HH}/k_{DD})_{obs}/[(k_{HH}/k_{RD})_{obs}(k_{HH}/k_{SD})_{obs}] \quad (4)$$

Deviation of this parameter from an ideal value of 1 serves as an experimental criterion for the existence of an electron transfer redox equilibrium in the rate-determining step, since on the basis of eqs 1−3, γ is given by eq 5 in the equilibrium SET model.

$$\gamma = (2\beta - 1)/\beta^2 \quad (5)$$

As shown in Table 4, the deviations of γ from unity do not appear to be statistically significant for most of the substrates that were tested, including benzyl and 4-methoxy benzyl alcohols, and 1-*O*-methyl-α-D-galactopyranoside, indicating that at least in those cases there is no need to invoke the existence of a redox equilibrium. However, for completeness, we report the value of the equilibrium isotope effect that is allowed by the data, and the consequence that the equilibrium isotope effect would have on the magnitude of the actual kinetic isotope effects. For the two substrates exhibiting a statistically significant deviation of γ from unity (4-nitro and 3-methoxy benzyl alcohols) (Table 4), the analysis leads to the prediction of relatively large equilibrium isotope effects (β) and inverse secondary kinetic isotope effects [α(2)′], raising questions about the validity of the apparent equilibrium isotope effect. In this context, it is important to note that galactose oxidase kinetics are particularly susceptible to artifacts arising from inhibitory impurities, since the enzyme may be inactivated (either reversibly or irreversibly) by reaction of the active site radical with minor components, and a small amount of inhibitory impurity in the (*S*)-[^{2}H]-benzyl alcohol samples (stoichiometric with enzyme) that is not offset by the presence of ferricyanide in the assay mixture could account for the observed behavior. The value of β shown here for the oxidation of galactose ($1/\beta = 0.78-0.8$) clearly justifies our previous analysis, although the fact that there is no consistent behavior over the five substrates suggests caution in the interpretation of an electron transfer redox equilibrium as an element of the galactose oxidase turnover mechanism.

Multiple Simultaneous Kinetic Isotope Effects. The complementary expression of solvent and substrate kinetic isotope effects has previously been reported as evidence for a shift

Table 4: Evaluation of Substrate Kinetic Isotope Effects within a Redox Equilibrium Model

substrate	γ^a	β^b	$\alpha(1)'^c$	$\alpha(2)'^d$
benzyl alcohol	0.99 ± 0.03	1.11 ± 0.03	4.8 ± 0.1	1.21 ± 0.04
4-nitro benzyl alcohol	0.90 ± 0.04	1.46 ± 0.05	7.3 ± 0.3	0.86 ± 0.04
4-methoxy benzyl alcohol	1.00 ± 0.03	1.00 ± 0.03	3.5 ± 0.1	1.19 ± 0.05
3-methoxy benzyl alcohol	0.93 ± 0.02	1.35 ± 0.04	2.85 ± 0.10	0.94 ± 0.03
1-*O*-methyl-α-D-galactopyranoside	0.95 ± 0.04	1.28 ± 0.05	10.2 ± 0.5	1.13 ± 0.05

[a] Defined as $\gamma = (k_{HH}/k_{DD})_{obs}/[(k_{HH}/k_{RD})_{obs}(k_{HH}/k_{SD})_{obs})]$. [b] Evaluated by solving eq 5 for β: $\beta = [1 \pm (1 - \gamma)^{1/2}]/\gamma$. [c] Apparent primary kinetic isotope effect for substrate oxidation $(k_{HH}/k_{SD})_{obs}$ corrected for the presence of an equilibrium isotope effect on electron transfer (β). [d] Apparent secondary kinetic isotope effect for substrate oxidation $(k_{HH}/k_{RD})_{obs}$ corrected for the presence of an equilibrium isotope effect on electron transfer (β).

Table 5: Multiple-Kinetic Isotope Analysis of the Galactose Oxidase Turnover Reaction

substrate	$(k_{H_2O}/k_{D_2O})_{HH}$	$(k_{H_2O}/k_{D_2O})_{DD}$	$(k_{HH}/k_{DD})_{H_2O}$	$(k_{HH}/k_{DD})_{D_2O}$
benzyl alcohol	1.17 ± 0.02	1.065 ± 0.04	7.12 ± 0.28	6.48 ± 0.19
4-nitro benzyl alcohol	1.07 ± 0.03	1.03 ± 0.02	11.8 ± 0.5	11.4 ± 0.3
4-methoxy benzyl alcohol	1.23 ± 0.02	1.07 ± 0.03	4.29 ± 0.09	3.73 ± 0.08

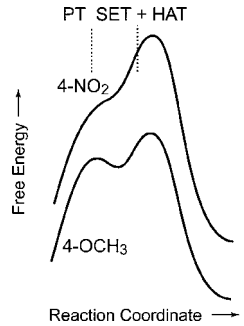

FIGURE 5: Hypothetical free energy reaction profiles for oxidation of benzyl alcohol by galactose oxidase. In the top trace, oxidation of 4-nitro benzyl alcohol is dominated by electron transfer and hydrogen atom transfer (SET+HAT), with no evidence for a proton transfer (PT) contribution in the rate-determining step. In the bottom trace, oxidation of 4-methoxy benzyl alcohol shows evidence for partially limiting PT in a stepwise mechanism.

in the nature of the rate-determining transition state from hydrogen atom transfer limiting (in the case of 4-nitro benzyl alcohol) to partially proton transfer limiting (in the case of 4-methoxy benzyl alcohol) (*22*). In these studies, we have extended this analysis by examining the effect of applying multiple simultaneous isotope perturbations (Table 5) as a test of the stepwise or concerted nature of the isotope-sensitive steps (*53*−*56*). For 4-nitro benzyl alcohol, there is virtually no detectable solvent kinetic isotope effect (SKIE) (*57*) for either α,α′-[^{1}H] or α,α′-[^{2}H] isotopomers, and the observed SKIE values are statistically identical. Similarly, the substrate KIE values are independent of the presence or absence of isotope in the solvent for this substrate. On the other hand, for benzyl alcohol, there is a small but statistically significant difference in the observed SKIE values depending on the labeling of the substrate, with the larger SKIE associated with the α,α′-[^{1}H] form of the substrate. In the same way, a small but statistically significant difference was observed for the substrate KIE value depending on the presence of isotope in the solvent, the larger KIE being associated with the unlabeled solvent (H_2O). An even larger variation in SKIE and KIE multiple isotope data is observed for 4-methoxy benzyl alcohol, with the same pattern of interdependences on the isotope perturbations. The small variations make the interpretation of these results problematic, but they are consistent with a picture in which the PT step becomes energetically resolved and kinetically significant with increasing electron-releasing character of the substituents in the benzyl alcohol series. An isotopic perturbation that makes a given step more rate-limiting decreases the rate-determining character of the other step, leading the pattern of interdependences that we observe. This allows a refinement of the catalytic reaction profile for benzyl alcohol oxidation as indicated in Figure 5.

CONCLUSIONS

Synthesis of a series of stereospecifically deuterated primary alcohol substrates for galactose oxidase has permitted the investigation of the substrate dependence of oxidation stereoselectivity for the first time. Galactose oxidase oxidizes galactose and benzyl alcohol derivatives with a wide range of rates but exhibits uniformly high (>95%) stereoselectivity for abstraction of the *pro-S* hydrogen of the substrate, with steric constraints on C_β of the substrate appearing to serve as a stereoselectivity determinant. Analysis of rate data for oxidation of (*R*) and (*S*) α-monodeuterated alcohols has allowed the substrate primary and secondary kinetic isotope effects to be resolved. The ratio of observed kinetic isotope effects measured with the α,α′-dideuterated substrate to the product of isotope effects observed for the (*R*) and (*S*) monodeuterated stereoisomers is defined as a parameter, γ, that serves as a criterion for the existence of an electron transfer redox equilibrium in the rate-determining step. A prior electron transfer equilibrium is permitted (but not required) by the experimental data. Multiple kinetic isotope studies have extended and refined the detailed mechanism of galactose oxidase, showing that for 4-methoxy benzyl alcohol the enzymatic oxidation mechanism involves stepwise proton abstraction and atom transfer, while for the other substrates that were tested, atom transfer dominates as the rate-limiting step in the reaction.

ACKNOWLEDGMENT

We thank the Reed College Chemistry Department for use of their NMR facility (supported by National Science Foundation Grant 0116373) and Dr. John Witte for insightful discussions. We also thank Lorne Isabelle (Mass Spectrometry Facilities, Department of Environmental and Biomo-

lecular Systems, Oregon Health and Sciences University) for expert assistance in the mass spectral analysis.

REFERENCES

1. Diner, B. A., and Rappaport, F. (2002) Structure, dynamics and energetics of the primary photochemistry of photosystem II of oxygenic photosynthesis, *Annu. Rev. Plant Biol. 53*, 551−580.
2. Gennis, R. B. (2004) Coupled proton and electron transfers in cytochrome oxidase, *Front. Biosci. 9*, 581−591.
3. Oubrie, A., and Dijkstra, B. W. (2000) Structural requirements of pyrroloquinoline quinone dependent enzymatic reactions, *Protein Sci. 9*, 1265−1273.
4. Anthony, C. (2001) Pyrroloquinoline quinone (PQQ) and quinoprotein enzymes, *Antioxid. Redox Signaling 3*, 757−774.
5. Gassner, G. T., Ludwig, M. L., Gatti, D. L., Correll, C. C., and Ballou, D. P. (1995) Structure and mechanism of the iron−sulfur flavoprotein phthalate dioxygenase reductase, *FASEB J. 9*, 1411−1418.
6. Stubbe, J., and van der Donk, W. A. (1998) Protein radicals in enzyme catalysis, *Chem. Rev. 98*, 705−762.
7. Frey, P. A. (1997) Radicals in enzymatic reactions, *Curr. Opin. Chem. Biol. 1*, 347−356.
8. Frey, P. A. (1990) Importance of organic radicals in enzymatic cleavage of unactivated C−H bonds, *Chem. Rev. 90*, 1343−1357.
9. Hamilton, G. A. (1982) Galactose oxidase and copper-containing amine oxidases, in *Copper proteins* (Spiro, T. G., Ed.) pp 193−218, Wiley Interscience, New York.
10. Kosman, D. J. (1984) Galactose oxidase, in *Copper proteins and copper enzymes* (Lontie, R., Ed.) Vol. 2, pp 1−26, CRC Press, Boca Raton, FL.
11. Villafranca, J. J., Freeman, J. C., and Kotchevar, A. (1993) Copper-containing enzymes: Structure and mechanism, *Bioinorg. Chem. Copper*, 439−446.
12. Whittaker, J. W. (2002) Galactose oxidase, in *Advances in Protein Chemistry* (Richard, A., and Gralla, E. B., Eds.) Vol. 60, pp 1−49, Academic Press, New York.
13. Whittaker, J. W. (2003) Free radical catalysis by galactose oxidase, *Chem. Rev. 103*, 2347−2363.
14. Whittaker, M. M., Kersten, P. J., Nakamura, N., Sanders-Loehr, J., Schweizer, E. S., and Whittaker, J. W. (1996) Glyoxal oxidase from *Phanerochaete chrysosporium* is a new radical-copper oxidase, *J. Biol. Chem. 271*, 681−687.
15. Whittaker, M. M., and Whittaker, J. W. (1988) The active site of galactose oxidase, *J. Biol. Chem. 263*, 6074−6080.
16. Ito, N., Phillips, S. E. V., Stevens, C., Ogel, Z. B., McPherson, M. J., Keen, J. N., Yadav, K. D. S., and Knowles, P. F. (1991) Novel thioether bond revealed by a 1.7 Å crystal structure of galactose oxidase, *Nature 350*, 87−90.
17. Whittaker, M. M., and Whittaker, J. W. (1993) Ligand interactions with galactose oxidase: Mechanistic insights, *Biophys. J. 64*, 762−772.
18. Reynolds, M. P., Baron, A. J., Wilmot, C. M., Vinecombe, E., Stevens, C., Phillips, S. E. V., Knowles, P. F., and McPherson, M. J. (1997) Structure and mechanism of galactose oxidase: catalytic role of tyrosine-495, *J. Biol. Inorg. Chem. 2*, 327−335.
19. Rogers, M. S., Baron, A. J., McPherson, M. J., Knowles, P. F., and Dooley, D. M. (2000) Galactose oxidase pro-sequence cleavage and cofactor assembly are self-processing reactions, *J. Am. Chem. Soc. 122*, 990−991.
20. Whittaker, M. M., and Whittaker, J. W. (2003) Cu(I)-dependent biogenesis of the galactose oxidase redox cofactor, *J. Biol. Chem. 278*, 22090−22101.
21. Whittaker, M. M., Ballou, D. P., and Whittaker, J. W. (1998) Kinetic isotope effects as probes of the mechanism of galactose oxidase, *Biochemistry 37*, 8426−8436.
22. Whittaker, M. M., and Whittaker, J. W. (2001) Catalytic reaction profile for alcohol oxidation by galactose oxidase, *Biochemistry 40*, 7140−7148.
23. Avigad, G., Amaral, D., Asensio, C., and Horecker, B. L. (1962) The D-galactose oxidase of *Polyporus circinatus*, *J. Biol. Chem. 237*, 2736−2743.
24. Maradufu, A., Cree, G. M., and Perlin, A. S. (1971) Stereochemistry of dehydrogenation by D-galactose oxidase, *Can. J. Chem. 49*, 3429−3437.
25. Choi, H., and Kuczkowski, R. L. (1985) Ozonolysis of styrene and *p*-nitrostyrene. Secondary deuterium kinetic isotope effects, *J. Org. Chem. 50*, 901−902.
26. Trahanovsky, W. S., Young, B., and Brown, G. L. (1967) Oxidation of organic compounds with cerium(IV). IV. Oxidation of benzyl and related alcohols, *J. Org. Chem. 32*, 3865−3868.
27. Midland, M. M., Tramontano, A., and Zderic, S. A. (1977) Preparation of optically active benzyl-α-*d* alcohol via reduction by *B*-3α-pinanyl-9-borabicyclo[3.3.1]nonane. A new highly effective chiral reducing agent, *J. Am. Chem. Soc. 99*, 5211−5213.
28. Midland, M. M., Greer, S., Tramontano, A., and Zderic, S. A. (1979) Chiral trialkylborane reducing agents. Preparation of 1-deuterio primary alcohols of high enantiomeric purity, *J. Am. Chem. Soc. 101*, 2352−2355.
29. Parker, D. (1983) ^{1}H and ^{2}H nuclear magnetic resonance determination of the enantiomeric purity and absolute conformations of α-deuteriated primary carboxylic acids, alcohols and amines, *J. Chem. Soc., Perkin Trans. 2*, 83−88.
30. Corey, E. J., and Suggs, J. W. (1975) Pyridinium chlorochromate. An efficient reagent for oxidation of primary and secondary alcohols to carbonyl compounds, *Tetrahedron Lett.*, 2647−2650.
31. Bollenback, G. N. (1963) Glycosidation: methyl α-D-glucopyranoside, in *Methods in Carbohydrate Chemistry* (Whistler, R. L., and Wolfrom, M. L., Eds.) Vol. 2, pp 326−328, Academic Press, New York.
32. Lewis, B. A., Smith, F., and Stephen, A. M. (1963) Methyl hydride reduction, in *Methods in Carbohydrate Chemistry* (Whistler, R. L., and Wolfrom, M. L., Eds.) Vol. 2, pp 68−76, Academic Press, New York.
33. Corey, E. J., Cho, H., Rücker, C., and Hua, D. H. (1981) Studies with trialkylsilyltriflates: new syntheses and applications, *Tetrahedron Lett. 22*, 3455−3458.
34. Stratton, J., Chiruvolu, V., and Meagher, M. (1998) High cell-density fermentation, *Methods Mol. Biol. 103*, 107−120.
35. Higgins, D. R., and Cregg, J. M. (1998) Introduction to *Pichia pastoris*, *Methods Mol. Biol. 103*, 1−15.
36. Whittaker, M. M., and Whittaker, J. W. (2000) Expression of recombinant galactose oxidase, *Protein Expression Purif. 20*, 105−111.
37. Tressel, P. S., and Kosman, D. J. (1982) Galactose oxidase from *Dactylium dendroides*, *Methods Enzymol. 89*, 163−171.
38. Whittaker, J. W., Lipscomb, J. D., Kent, T. A., and Munck, E. (1984) *Brevibacterium fuscum* protocatechuate 3,4 dioxygenase. Purification, crystallization and characterization, *J. Biol. Chem. 259*, 4466−4475.
39. Patil, P. V., and Ballou, D. P. (2000) The use of protocatechuate 3,4 dioxygenase for maintaining anaerobic conditions in biochemical experiments, *Anal. Biochem. 286*, 187−192.
40. Sweeley, C. C., Bentley, R., Makita, M., and Wells, W. W. (1963) Gas−liquid chromatography of trimethylsilyl derivatives of sugars and related substances, *J. Am. Chem. Soc. 85*, 2497−2507.
41. Brown, H. C., and Singaram, B. (1988) Development of a simple general procedure for synthesis of pure enantiomers via chiral organoboranes, *Acc. Chem. Res. 21*, 287−293.
42. Ohrui, H., Nishida, Y., and Meguro, H. (1984) The synthesis of D-(6*R*)- and (6*S*)-(6-^{2}H$_{1}$)-galactose, *Agric. Biol. Chem. 48*, 1049−1053.
43. Nishida, Y., Ohrui, H., and Meguro, H. (1984) ^{1}H-NMR strudies of (6*R*)- and (6*S*)-deuterated D-hexoses: assignment of the preferred rotamers about the C5−C6 bond of D-glucose and D-galactose derivatives in solution, *Tetrahedron Lett. 25*, 1575−1578.
44. Lambert, J. B., and Greifenstein, L. G. (1973) Stereochemical dependence of the chemical-shift isotope effect, *J. Am. Chem. Soc. 95*, 6150−6152.
45. Sun, D., Ono, K., Okajima, T., Tanizawa, K., Uchida, M., Yamamoto, Y., Mathews, F. S., and Davidson, V. L. (2003) Chemical and kinetic reaction mechanisms of quinohemoprotein amine dehydrogenase from *Paracoccus denitrificans*, *Biochemistry 42*, 10896−10903.
46. Wachter, R. M., and Branchaud, B. P. (1998) Construction and analysis of a semi-quantitative energy profile for the reaction catalyzed by the radical enzyme galactose oxidase, *Biochim. Biophys. Acta 1384*, 43−54.
47. Himo, F., Eriksson, L. A., Maseras, F., and Siegbahn, P. E. M. (2000) Catalytic mechanisms of galactose oxidase: A theoretical study, *J. Am. Chem. Soc. 122*, 8031−8036.
48. Mayer, J. M. (2004) Proton-coupled electron transfer: a reaction chemist's view, *Annu. Rev. Phys. Chem. 55*, 363−390.
49. Cleland, W. W. (2003) The use of isotope effects to determine enzyme mechanisms, *J. Biol. Chem. 278*, 51975−51984.

50. Melander, L., and Saunders, W. H., Jr. (1987) *Reaction Rates of Isotopic Molecules*, Krieger Publishing Co., Malabar, FL.
51. Frantom, P. A., Pongee, R., Sulikowski, G. A., and Fitzpatrick, P. F. (2002) Intrinsic deuterium isotope effects on benzylic hydroxylation by tyrosine hydroxylase, *J. Am. Chem. Soc. 124*, 4202−4203.
52. Cleland, W. W. (1980) Measurement of isotope effects by the equilibrium pertubation technique, *Methods Enzymol. 64*, 104−125.
53. Cleland, W. W. (1991) Multiple isotope effects in enzyme-catalyzed reactions, in *Enzyme Mechanism from Isotope Effects* (Cook, P. F., Ed.) pp 247−265, CRC Press, Boca Raton, FL.
54. Hermes, J. D., Roeske, C. A., O'Leary, M. H., and Cleland, W. W. (1982) Use of multiple isotope effects to determine enzyme mechanisms and intrinsic isotope effects. Malic enzyme and glucose-6-phosphate dehydrogenase, *Biochemistry 21*, 5106−5114.
55. Belasco, J. G., Albery, J. A., and Knowles, J. R. (1983) Double isotope fractionation: Test for concertedness and for transition state dominance, *J. Am. Chem. Soc. 105*, 2475−2477.
56. Sobrado, P., and Fitzpatrick, P. F. (2003) Solvent and primary deuterium kinetic isotope effects show that lactate CH and OH bond cleavages are concerted in Y254F flavocytochrome b_2, consistent with a hydride transfer mechanism, *Biochemistry 42*, 15208−15214.
57. Schowen, K. B., and Schowen, R. L. (1982) Solvent isotope effects of enzyme systems, *Methods Enzymol. 87*, 551−606.

BI048554S